

Electronic Supplementary Information

Dynamics of nanocrystal structure and composition in growth solutions monitored by *in situ* lab-scale X-ray diffraction

*Helena Fridman, Michael Volokh and Taleb Mokari**

*Department of Chemistry and Ilse Katz Institute for Nanoscale Science and Technology, Ben-Gurion University of the Negev, Beer-Sheva, 8410501, Israel
E-mail: mokari@bgu.ac.il*

Additional experimental methods

Calculation of grain size using a Scherrer analysis

The full-width at half-maximum, FWHM, (β_{Total}) and diffraction angle (θ_β), which were obtained from the XRD profile fitting were used to calculate the grain size (L), which corresponds to the {002} and {101} planes of CdS. The calculation was performed using the Scherrer equation:

$$L = \frac{\kappa\lambda}{\beta_{Total}\cos(\theta_\beta)}$$

Where κ is the shape factor, taken as 0.9, and λ is the experimental incident X-ray wavelength (1.5405 Å). The same calculation was performed on all three repeats of the *in situ* growth of CdS in oleylamine (OLAM), and the averaged result with the standard deviation is plotted in Fig. 2a.

To evaluate the contribution of instrumental broadening (β_{Inst}) to the measured sample broadening (β_{Total}), we ran a measurement of a standard compound, NIST® SRM® 660c LaB₆, using the same instrument and experimental settings. The contribution of the sample to the total broadening (β_{Sample}) was calculated as:

$$\beta_{Sample} = \sqrt{\beta_{Total}^2 - \beta_{Inst}^2}$$

The result after the correction had a negligible effect on the measured value (less than 0.01 % deviation) Therefore, β_{Total} was directly used for grain size evaluation.

Composition determination using Vegard's law (Cd mole fraction in Cd_xZn_{1-x}S solid solutions)

The Cd-mole fraction (x) of Cd_xZn_{1-x}S may be calculated using Vegard's law,^[1] and it was applied on the lattice parameter c at each timeframe of the experiment. First, the lattice parameter of the alloyed NPs ($c_{Cd_xZn_{1-x}S}$) was calculated based on the (002) peak position. Then, the calculation of x was as follows:

$$c_{Cd_xZn_{1-x}S} = (1-x) \cdot c_{CdS} + x \cdot c_{ZnS}$$

Where c_{CdS} and c_{ZnS} are the c lattice parameters of wurtzite CdS and ZnS phases, respectively. The lattice parameters were taken from ICDD JCPDS card no. 41-1049 and 36-1450, respectively. The calculated x as function of time for all different Cd/Zn precursor ratios is presented in Fig. 4b.

In situ time-resolved X-ray diffraction (TR-XRD) data fitting and calculations

In situ TR-XRD patterns were fitted using *Match! 3.11.3.192* software. Background flexibility was set to two, and the sensitivity of profile fitting and the default full width at half maximum

(FWHM) was determined automatically. The calculated pattern is presented on top of the experimental data in Fig. 1, 3, S2b, S3, and S7a. The FWHM and the peak position obtained from XRD profile fitting was used to calculate the grain size of CdS and the Cd-mole fraction of $\text{Cd}_x\text{Zn}_{1-x}\text{S}$, as described below. For more details on the fitting parameters, see screenshot from the *Match!* software in Fig. S1.

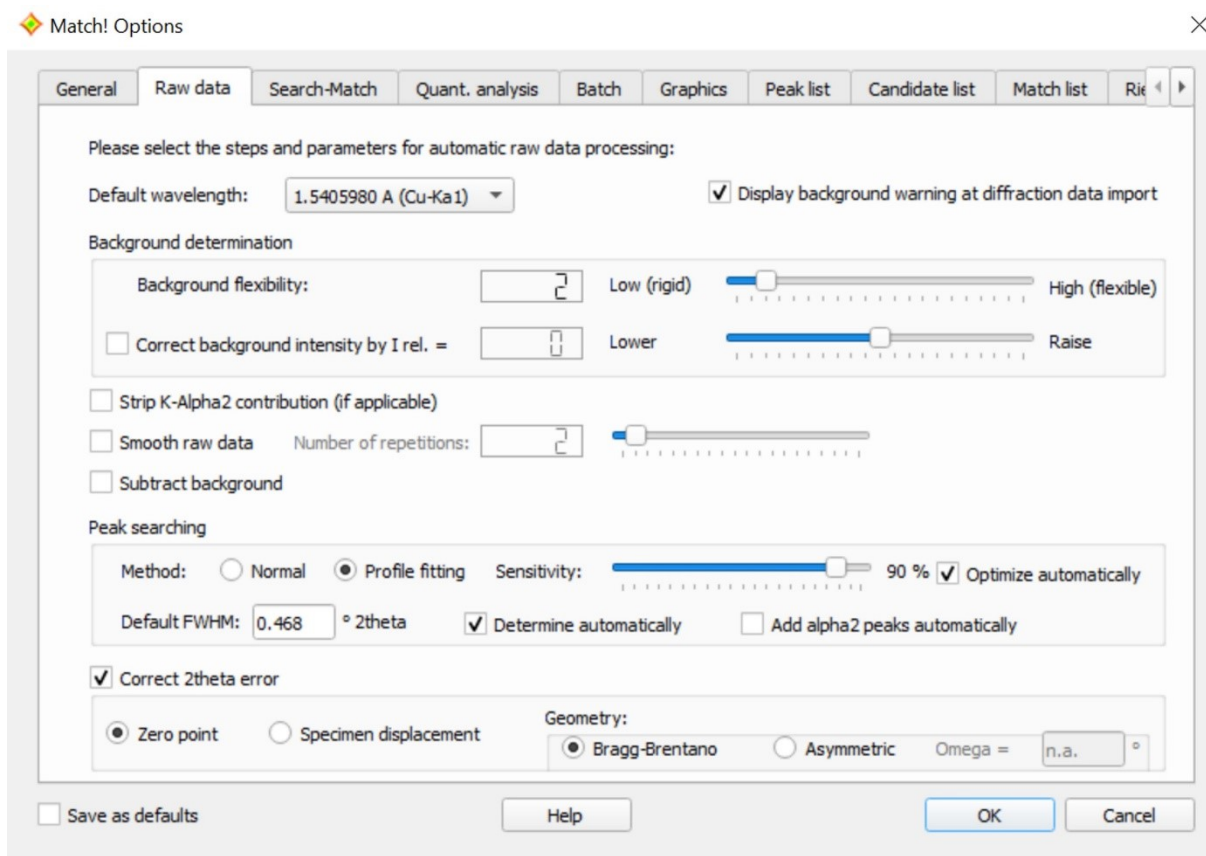


Fig. S1 A screenshot of the experimental data fitting parameters in *Match!*

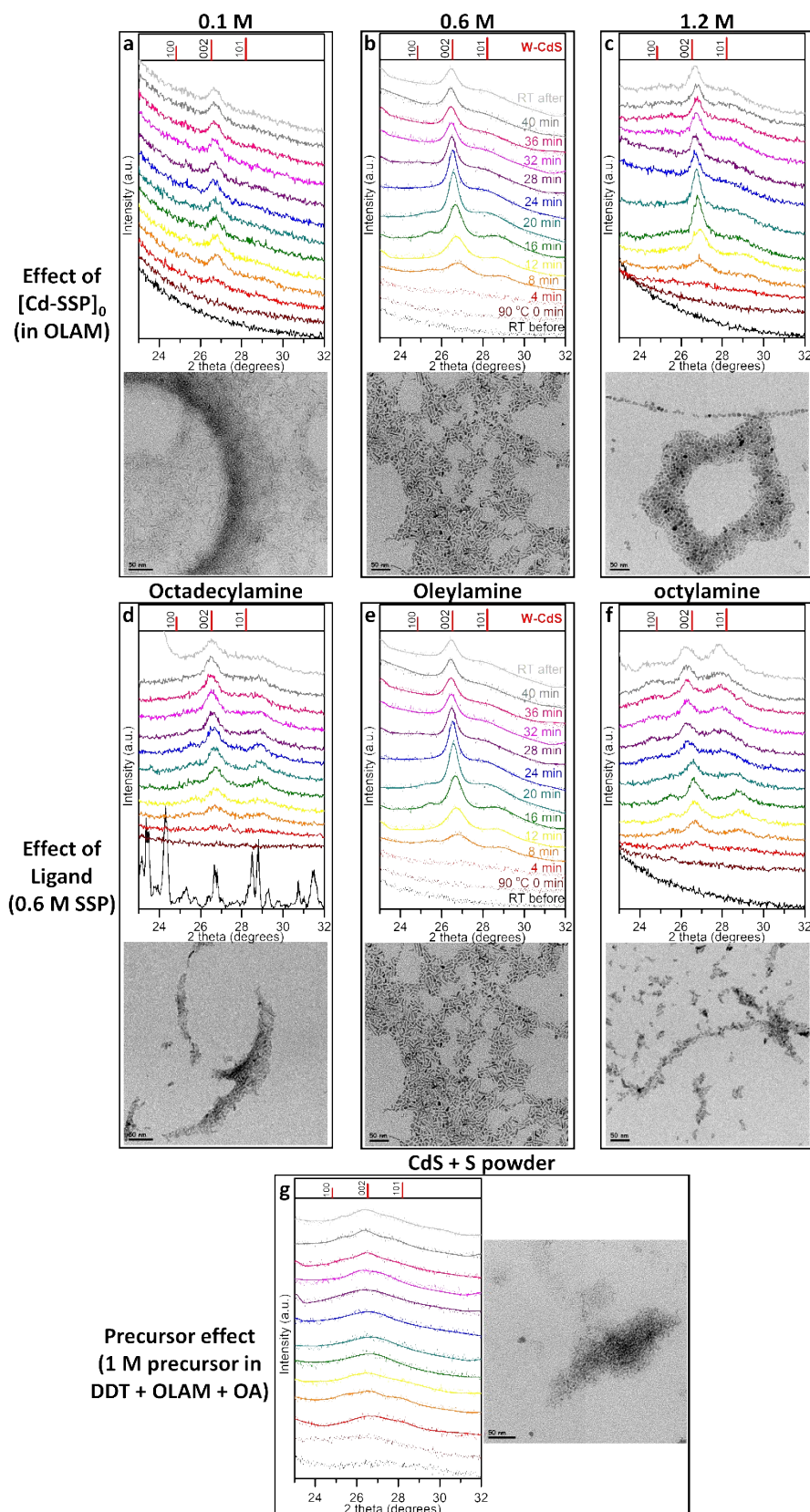


Fig. S2 *In situ* TR-XRD of CdS NP formation under different reaction concentrations (a-c), ligands (d-f) and precursors (g) with the corresponding TEM images of the final products below/on the right. Reaction parameters are stated on top of each pattern and on the left. The temperature and time are mentioned above the XRD patterns of 0.6 M SSP in OLAM; the correlation between the color-code and time applies to all other patterns.

DDT = dodecanethiol and OA = oleic acid.

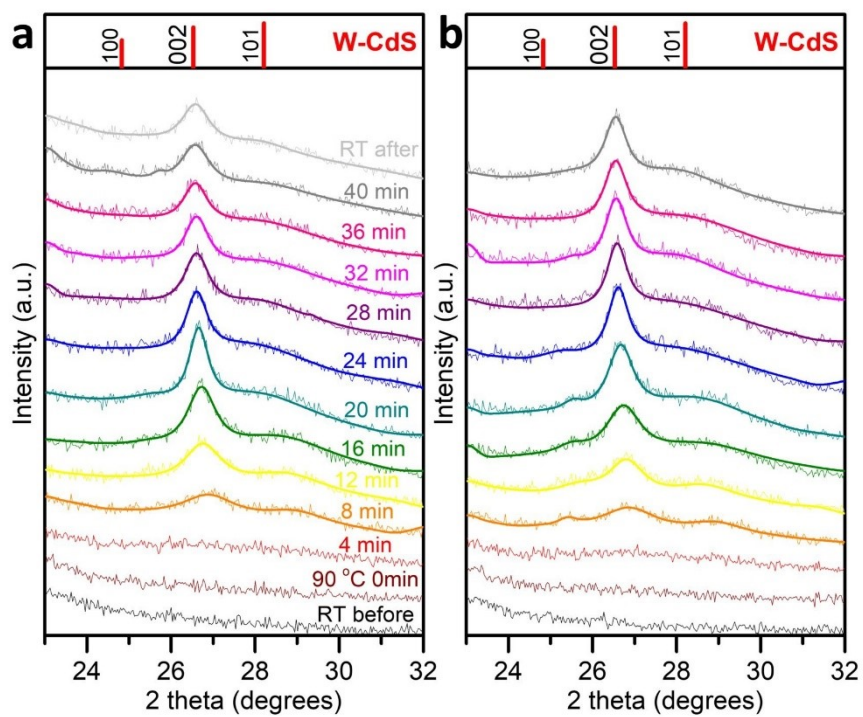


Fig. S3 Two additional repeats of the *in situ* TR-XRD of CdS formation from 0.6 M SSP ($[\text{Cd}(\text{dteEt}_2)_2]$) in OLAM at 90 °C. The starting measurement time is stated above each pattern in (a); the correlation between the color-code and time applies to both (a) and (b).

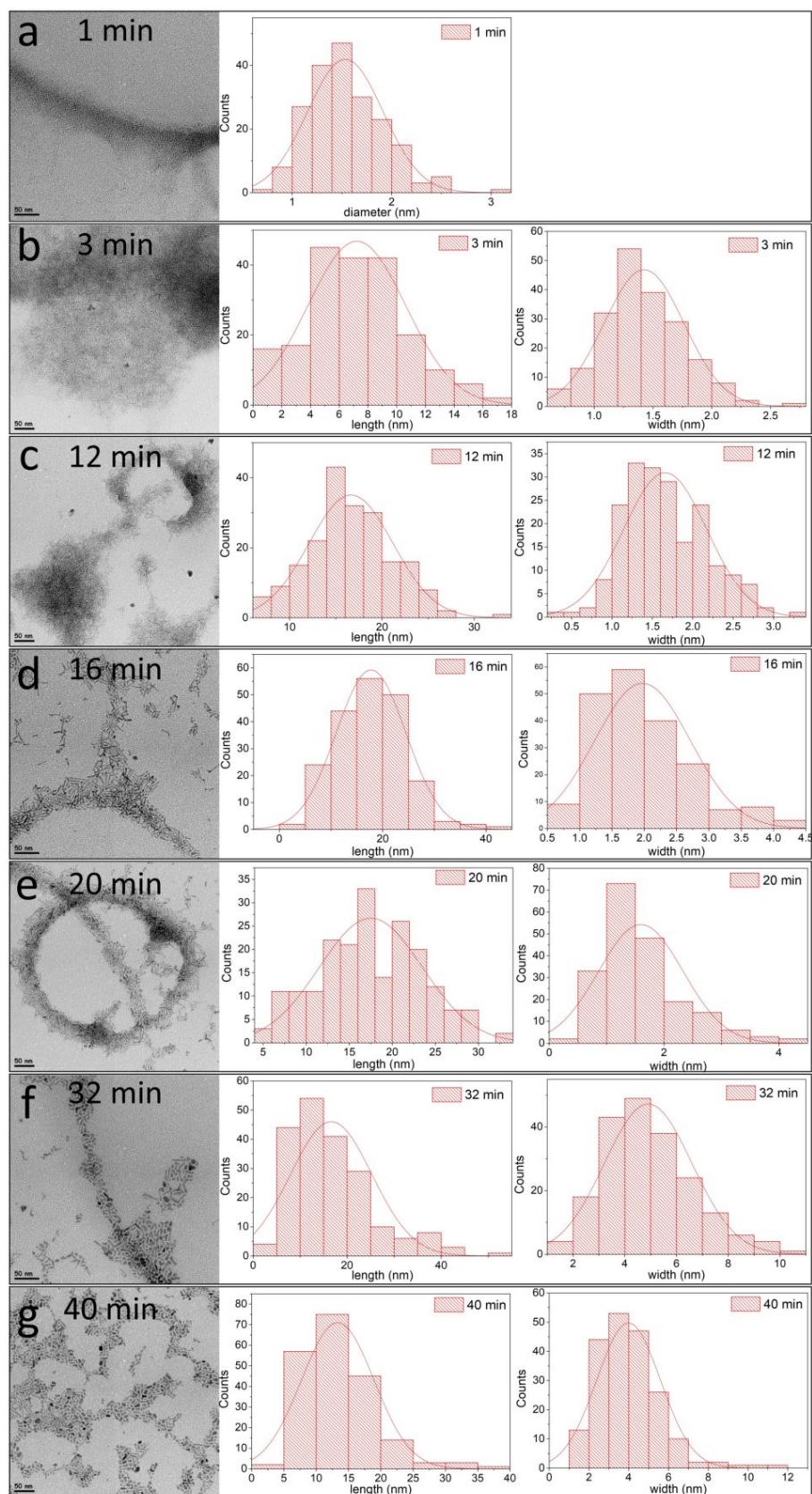


Fig. S4 Representative TEM images of an *ex situ* experiment of CdS growth and the corresponding size histograms of the resultant NPs as measured from 200 NPs; left column—TEM, middle column—length, right column—width. (a), (b), (c), (d), (e), (f), and (g) correspond to aliquots taken after 1, 3, 12, 16, 20, 32, and 40 minutes of the reaction.

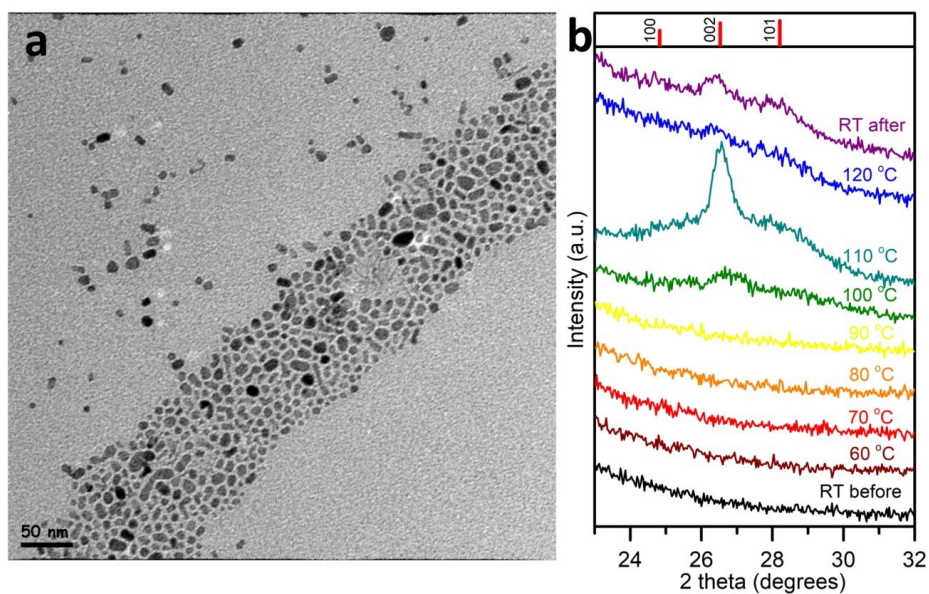


Fig. S5 (a) TEM and (b) *in situ* XRD of CdS synthesized at higher reaction temperatures, which allows reaching a more advanced stage of digestive ripening. In the same manner as in Fig. 2, the intensity of diffractions attributed to the (002) plane first increases and then decreases with reaction progress (time).

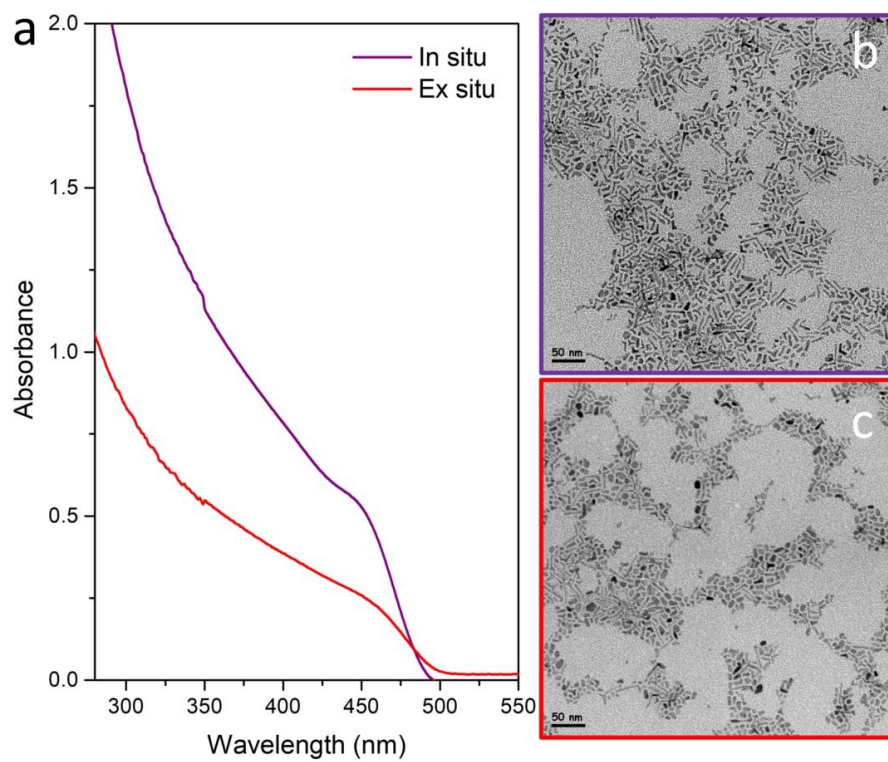


Fig. S6 Comparison between the UV-vis spectra (a) and TEM measurement of the final products of CdS synthesized *ex situ* (b) and *in situ* (c). Scale bars are 50 nm.

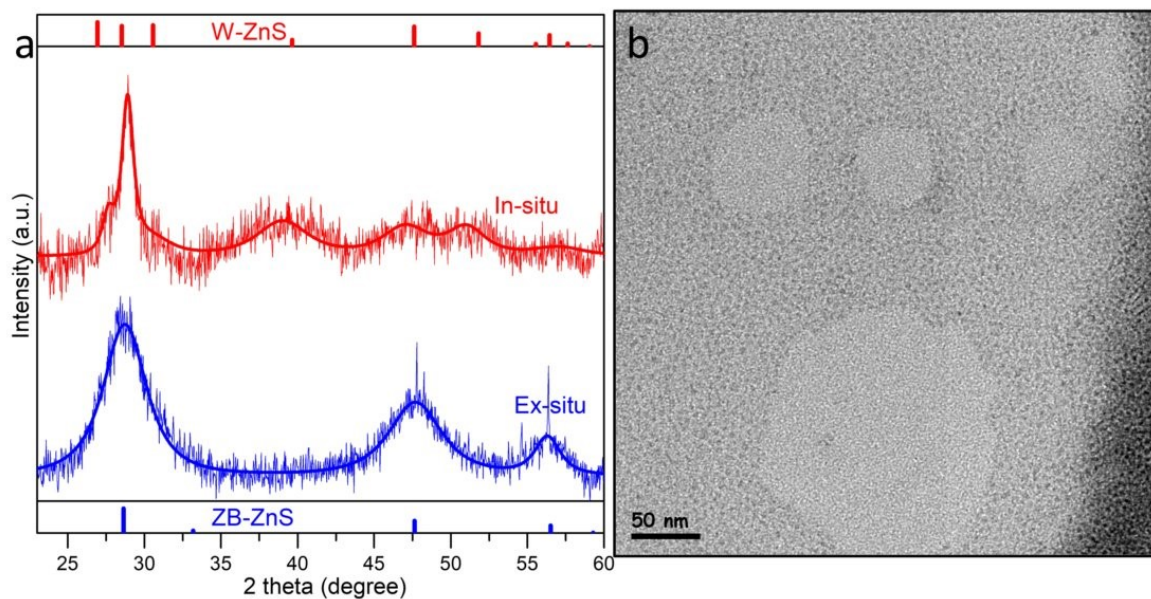


Fig. S7 *In-situ* XRD of ZnS NPs synthesized from 1.2 M SSP ($[\text{Zn}(\text{dteEt}_2)_2]$) in OLAM at 90 °C. (a) XRD; top pattern is the product measured in the growth solution (*in situ*), and bottom pattern is the same product after precipitation with hexane and ethanol and centrifugation followed by redispersion in hexane and drop-casting on a Si substrate (*ex situ*). A significant phase transformation from wurtzite to zinc blende phase is observed in *ex situ* compared to the *in situ*. (b) TEM image, corresponding to the final product of *in situ* TR-XRD. ICDD JCPDF card numbers 36-1450 and 65-0309 were used for the literature data of wurtzite (W) and zinc blende (ZB) ZnS, respectively, shown as stick patterns in (a).

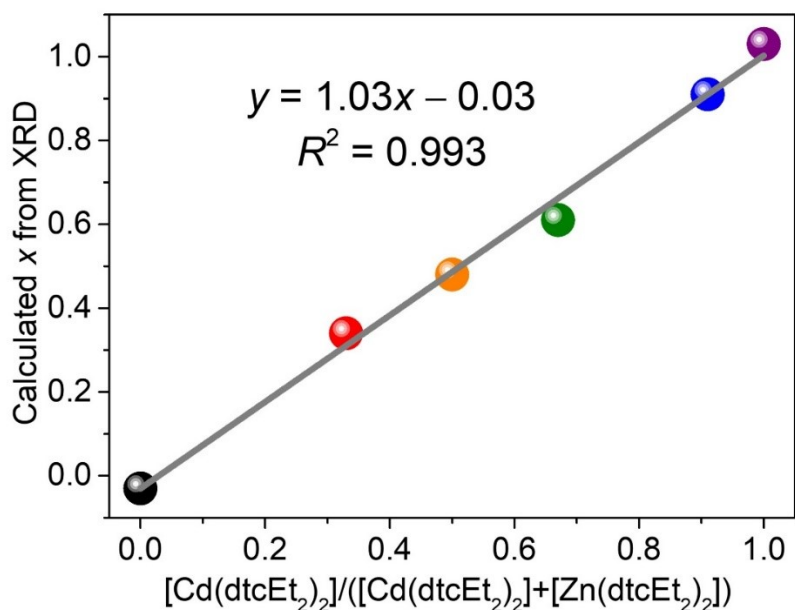


Fig. S8 Calculated x in the $\text{Cd}_x\text{Zn}_{1-x}\text{S}$ products based on the XRD data (analysis using Vegard's law) vs. the initial mole fraction of $[\text{Cd}(\text{dtcEt}_2)_2]$ out of the total precursor mixture (*i.e.*, experimental values in the final products vs. theoretical values based on initial precursor ratio). The good linear fit ($ax + b$, with a close to unity and b close to 0) of the correlation between the two parameters indicates that the starting Cd/Zn SSP ratio is similar to the final Cd/Zn ratio in the $\text{Cd}_x\text{Zn}_{1-x}\text{S}$ product alloy NPs.

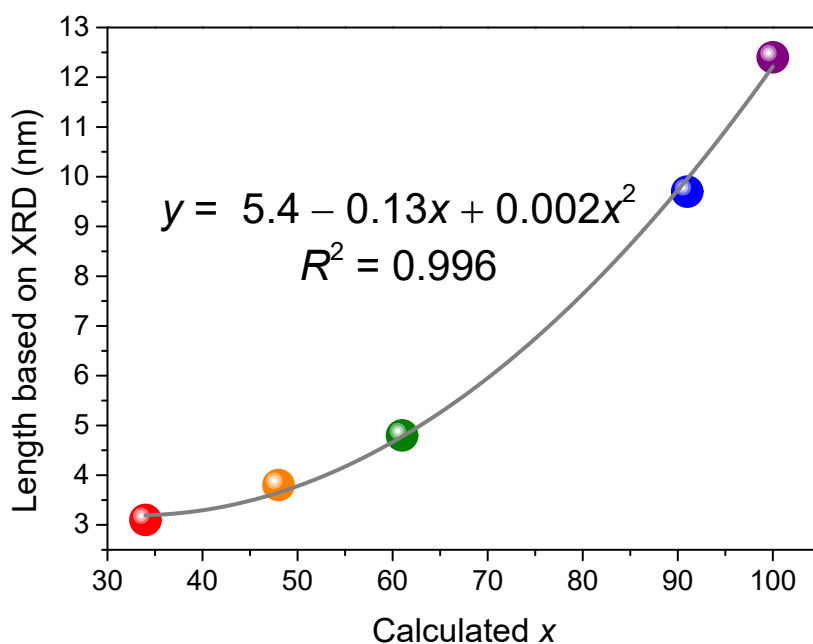


Fig. S9 Calculated length of the $\text{Cd}_x\text{Zn}_{1-x}\text{S}$ product NPs based on TR-XRD plotted against the corresponding calculated x .

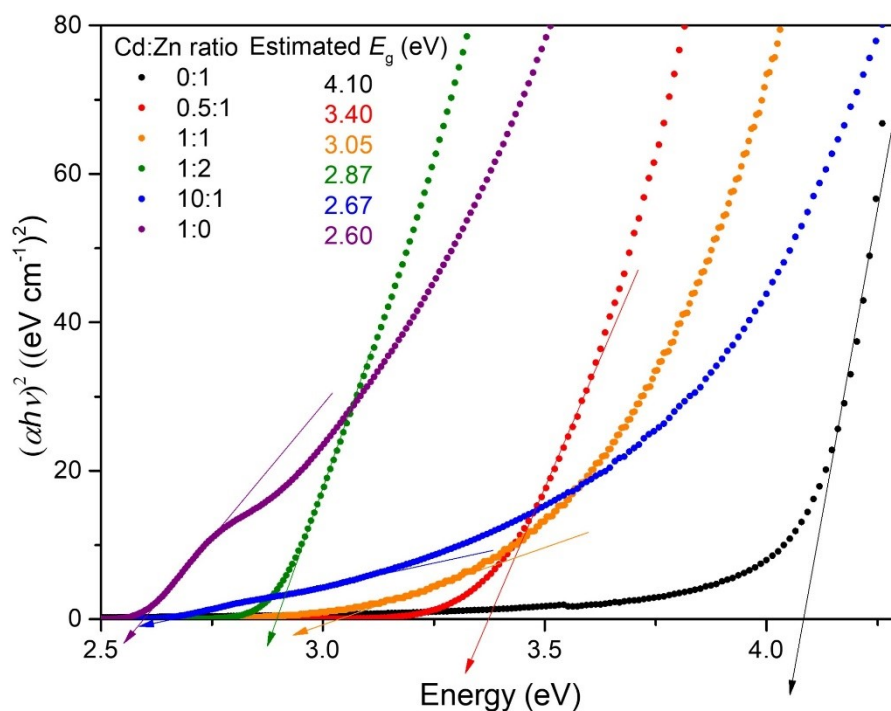


Fig. S10 Tauc plot analysis of the different Cd:Zn precursor ratios calculated from the UV–vis absorption spectra to determine the direct band gap (E_g) of $\text{Cd}_x\text{Zn}_{1-x}\text{S}$.

Tauc plots were obtained by $(\alpha h\nu)^{1/n}$ as a function of $h\nu$ (the photon energy), where $\alpha = 2.303A$ (α is the absorption coefficient and A is the absorbance). For CdS, ZnS, and $\text{Cd}_x\text{Zn}_{1-x}\text{S}$ solid solutions, $n = 1/2$ since these materials have a direct band gap.¹

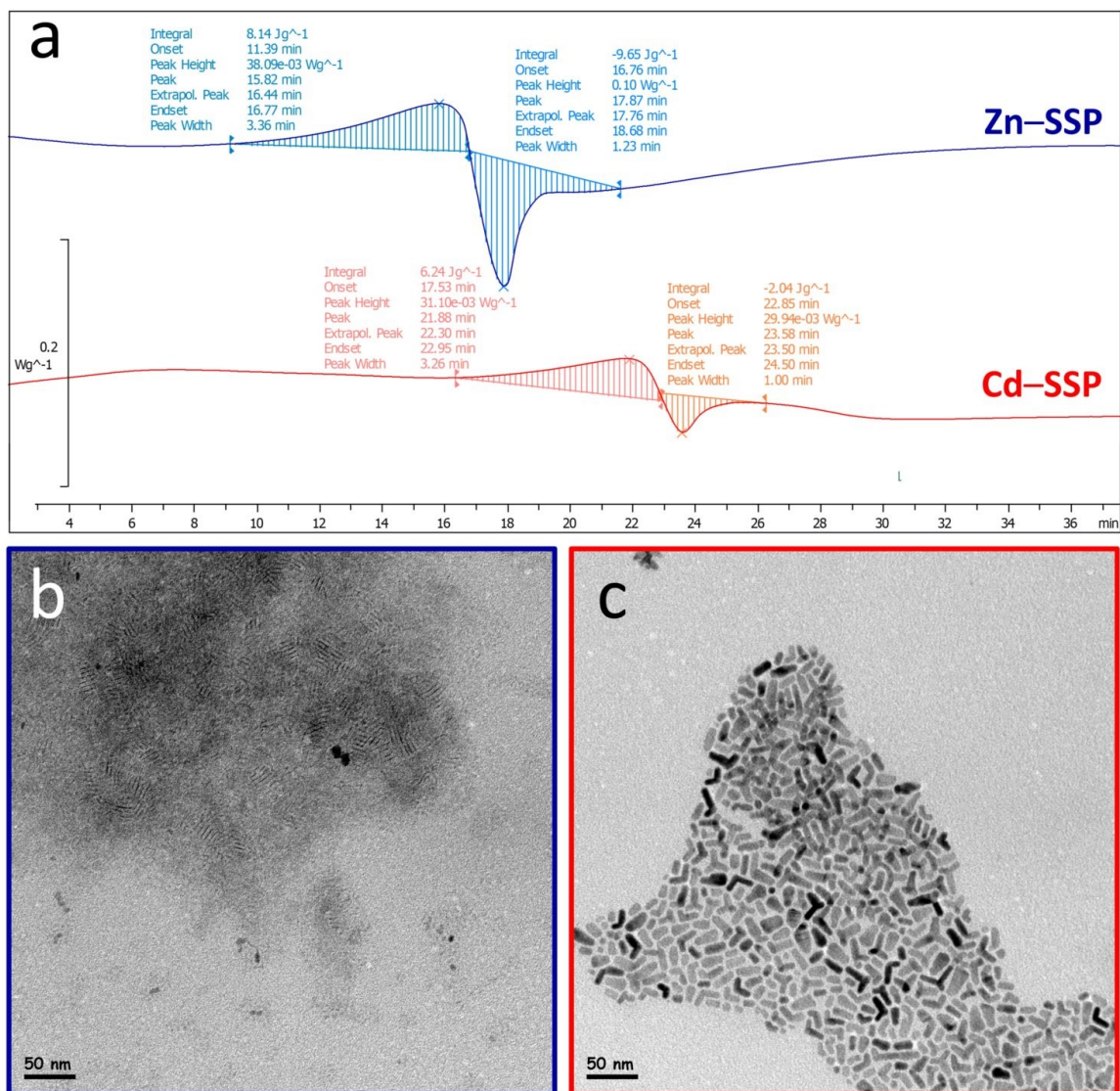


Fig. S11 (a) DSC curves of 0.6 M Zn- and Cd-SSPs ($[M(\text{dteEt}_2)_2]$, $M = \text{Zn, Cd}$), decomposed in OLAM at 90 °C, and the corresponding TEM images of the final products of (b) $[\text{Zn}(\text{dteEt}_2)_2]$ and (c) $[\text{Cd}(\text{dteEt}_2)_2]$ decomposition in OLAM (taken from washed and redispersed product from the DSC crucible).

Electronic Supplementary Information References

- 1 M. Volokh, M. Diab, O. Magen, I. Jen-La Plante, K. Flomin, P. Rukenstein, N. Tessler and T. Mokari, *ACS Appl. Mater. Interfaces*, 2014, **6**, 13594–13599.